International Journal of Research and Reviews in Wireless Communications (IJRRWC)
Vol. 1, No. 3, September 2011, ISSN: 2046-6447

www.sciacademypublisher.com

A Novel Design of Phased Antenna Array Based on Digital Beamforming

Ridha Ghayoula[1], Najib Fadlallah[2], Bertand Granado[3], Ali .Gharsallah[1], and Mohamed Rammal[2]

[1]Faculty of Mathematical, Physical and Natural Sciences of Tunis, Department of Physic, El Manar University, Tunisia
[2]RADIOCOM Team, High Institute of Technology Saida, Lebanon
[3]ETIS-ENSEA, Cergy-Pontoise University, Paris-France

Email: ridha.ghayoula@fst.rnu.tn

Abstract –The phased antenna array consists of a combination of multiple antenna elements with a signal-processing capability to optimize its radiation and/or reception pattern automatically in response to the signal environment. In a telecommunication, the phased antenna array is the port through which radio frequency (RF) energy is coupled from the transmitter to the environment and, in reverse, to the receiver from the environment. In this paper, a novel design of phased antenna array based on digital beamforming is proposed. The goal of the design is to construct smart antenna beamforming systems with hardware-software implemented neural network. A newly proposed synthesis method is used to design antenna arrays capable of delivering a much better radiation performance in terms of homogenous coverage and reduced interference with phased arrays and capable to beamforming and electronic steering by adjusting the relative phases of the signal received or transmitted by each antenna. To verify the performances of the proposed technique, an 8-element array has been realized and tested for various types of beam configurations.

Keywords – Neural network, back-propagation algorithm, synthesis method, phased antenna array, Steering beams, multiple steering, Interference nulling

1. Introduction

IN RECENT years, wireless communication systems have progressed greatly and the market, especially for the cellular phone, has witnessed explosive growth. Moreover, as the demand for multimedia services increases, a wider bandwidth of information will be required for next generation wireless systems [1]. These systems will be allocated at a higher frequency band because a number of useful frequency bands have already been allotted to and are occupied by existing systems. In order to accommodate a larger number of subscribers and to provide better quality services, it is necessary to increase the channel capacity. Further, the technologies required for power saving and efficient frequency reusability will be necessary for various multimedia services. The efficient use of the frequency resources is necessary to achieve higher data transmission throughput. Smart antenna systems are capable of automatically changing the directionality of their radiation patterns in response to their signal environment. This can noticeably improve the performance characteristics, such as channel capacity and quality of a wireless system. Smart antenna systems, by using spatially separated antennas, referred to as antenna array, maximize the Signal-to-Interference-plus-Noise Ratio (SINR) of the received signals, and suppress interferences and noise power by digital signal processing after analog to digital conversion [2].

Conventional antenna systems, which employ a single antenna, radiate and receive information equally in all directions. This omni-directional radiation leads to the distribution of energy in all directions. This wasted power becomes a potential source of interference for other users or for other base stations in other cells. Interference and noise reduce the Signal-to-Noise Ratio (SNR) used for detection and demodulation, resulting in poor signal quality. Today's cellular systems usually introduce 120° sectorization of the coverage to enhance capacity [3].

On the other hand, smart antennas at the transmitter are capable of steering the maximum radiation pattern toward the desired mobile at the receiver; they can spatially separate the energy of the interference [4-6] and mitigate multipath fading using a software algorithm. This ensures that an optimum quality of service is delivered to users, and it provides maximum coverage for a base station. Smart antennas can use spatial domain processing by using multiple antennas, thus enabling them to have intelligence to process the data at both receiver and transmitter [9]. The smart antennas are often classified as switched-beam arrays and adaptive array antennas. The switched-beam arrays comprise beamforming networks and a beam selection processor. The processor selects the beam with maximum power response by switching the beams. However, the adaptive array antennas incorporate more intelligence than the switched beam arrays. Adaptive array antennas can estimate their environment in accordance with the propagation channel responses between the receiver and the transmitter. This information is then used to weigh the data received at/transmitted from the antenna array to maximize the response for the desired user. The processor determines the optimum weight vector.

In [3] the author's describes prototyping of a neuroadaptive smart antenna beamforming algorithm using hardware-software implemented RBF (Radial- Basis-

Function neural network) and Field Programmable Gate Array system-on-programmable-chip (SoPC) approach. In [7] the author's presents the array factor of a phased array antenna driven by a chirped fiber Bragg grating.

In this study, we focus on adaptive beamforming algorithms with a general approach, by phase only adjustment to synthesis desired beam and multibeam with interfering steered. The basic idea of the present approach is to apply the two terms of Madsen expansion to express a steering vector in a particular direction [8]. To construct a set of linear equations that can be optimized with minmax criterion. The resulting linear system can be solved in the minmax sense by a method similar to Madsen algorithm [9].

Thanks to this formulation, we are able to steer beams and nulls at the desired direction, and at the same time keep the average side lobe level at its minimum. The technique proposed in this paper is based on neural network and back-propagation technique to synthesis steered beams with interfering in desired direction and steering lobes in the directions of the different users by phase control. The generalization represents the Newton for the constrained case. They are considered as one of the most efficient general purpose nonlinear programming algorithms today. The basic principle of Neural Networks model is used to replace the given nonlinear problem.

The paper is organized as follows. The synthesis problem formulation is presented in section II. Multilayer Networks And Back-Propagation Algorithm is developed in section III. Section IV shows the novel design of phased antenna array with the simulation and measurement result, finally, section V makes conclusions.

2. Synthesis Problem Formulations

Mathematically, the purpose of numerical synthesis techniques is to minimize the error between the required radiated function and the computed one. The algorithm is based on successive linear approximation to the nonlinear functions defining the problem [5]-[9]; the resulting linear systems are solved in the minmax sense. The results obtained are an equiripples radiation patterns. The obtained beams have equal relative errors (equal decibel ripples) in the pattern region and equal side lobes in the side -lobe region.
The angular behaviour of the far field E of a linear spaced array of 2N equi-amplitude radiators can be written as [10-5]:

$$E_c\left(\theta_j\right)=\frac{1}{2N}\sum_{n=1}^{2N} e^{j\left(k_0 x_n \sin\left(\theta_j\right)+\varphi_n\right)} \qquad (1)$$

In (1), k_0 is the wavelength; x_n is the spacing between the two elements; θ_j is the elevation angle; and φ_n the phase excitation (Fig.1).

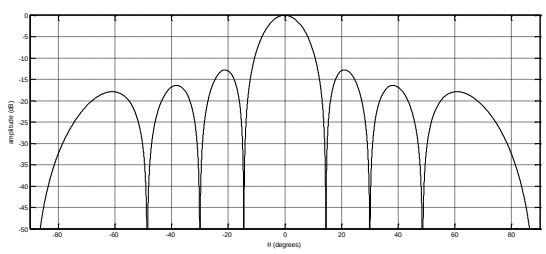

Figure 1. $E_c\left(\theta\right)$ with (N=8 and $x_n=\frac{\lambda}{2}$).

Desired patterns are usually defined in amplitude, and optimal realizable patterns can only be defined with respect to some error criterion. We will consider the minmax norm, defined as the minimization of the function:

$$Err\left(\theta_j\right)=W_j.Max_{\substack{j=1,...,M}}\left\|\left|E_c\left(\theta_j\right)\right|-\left|E_d\left(\theta_j\right)\right|\right\| \qquad (2)$$

Where E_c is the variable far field and E_d is desired far filed or desired radiation pattern.

Under the constraints:

$$W_i.\left\|\left|E_c\left(\theta_i\right)\right|-1\right\|=0 \qquad (3)$$

Where θ_i is the angular position of the main lobes.

$$W_k.\left\|E_c\left(\theta_k\right)\right\|=0 \qquad (4)$$

Where θ_k is the angular position of the side lobes.

M is the number of the sampled angular direction, E_d is the normalized amplitude of the required pattern field, and E_d is the amplitude of calculate pattern field (power synthesis) [10]. Error weighting $\left(W_j\right)$ in each direction can be adjusted to specify the desired levels of array pattern. This property may be used to synthesize the beam in all possible directions and to cancel interfering sources operating at the same frequency as that of the desired source, providing a spatial separation, which is large enough.

In the case of power synthesis, the error to minimize is equal to the difference between the modulus of the computed function and the required one. It is proved that the real synthesis is preferable in case of directive beam. In the real field synthesis case, calculated field is real, and the excitation distribution is symmetrical and conjugated with the array centre. The computed fields become:

$$E_c\left(\theta_j\right)=\frac{1}{N}\sum_{n=1}^{N}\cos\left(k_0 x'_n \sin\left(\theta_j\right)+\varphi_n\right) \qquad (5)$$

With x'_n, the relative position of the nth element with the array center [5].
The method of optimization nonlinear seeks to solve the system of nonlinear equations:

$$ERR(\underline{x},\theta_j)=0 \qquad \text{j=1,…,M} \qquad (6)$$

Within the meaning of minmax where it is a question of finding vector $\underline{x}$ of synthesis parameters, which minimizes the maximum of the function error:

$$\overline{ERR}(\underline{x})=\max_j\left\|ERR(\underline{x},\theta_j)\right\|^2 \quad \text{j=1,…,M} \qquad (7)$$

The followed approach consists in approximating the nonlinear function for which one can calculate under gradient in any point, by tangential linearization, then to refine the approximation repeatedly. One is thus brought to solve a system of linear equations to which constraints can be added progressively with the iterations, to ensure the convergence of the method.

With the iteration $k+1$, vector $\underline{x}(k+1)$ is written

$$\underline{x}(k+1) = \underline{x}(k) + \underline{h}(k) \quad \text{with} \quad \underline{h}(k) = (h_1,\ldots,h_n) \tag{8}$$

Optimization relates to the system of equations linearized where $h(k)$ is the solution which minimizes the maximum of the function of linearized error:

$$\overline{ERR}(\underline{h}(k),\theta_j) = ERR(\underline{x}(k),\theta_j) + grad(ERR(\underline{x}(k),\theta_j).\underline{h}(k)) \quad j=1,\ldots,M \tag{9}$$

Must satisfy a certain contraint:

$$\max_{i=1,\ldots,n} \left\|h_i\right\| \le \lambda(k) \tag{10}$$

The search for a minimum of the linear system is equivalent to the traditional problem of optimization.

$$Min\ \hat{ERR}(\underline{h}(k)) = \sum_{i=1}^{N} a_i h_i \tag{11}$$

Under the contraints

$$\overline{ERR}(\underline{h}(k)) \le ERR(\underline{x}(k),\theta_j) \qquad j=1,\ldots,M$$
$$\left\|h_i\right\| \le \lambda(k) \qquad i=1,\ldots,N \tag{12}$$

Where

$$\hat{ERR}(\underline{h}(k)) = \max_j \left| ERR(\underline{x}(k),\theta_j) + grad(ERR(\underline{x}(k),\theta_j).\underline{h}(k) \right| \tag{13}$$

Desired patterns are usually not realisable, and an optimal realisable pattern can only be defined with respect to some error criterion. We will consider the linear approximation and minmax norm, defined as eq.14.

The function $(\overline{ERR}(\underline{x}(k))$ exceeds a fraction of the decrease of the maximum of the function linearized:

$$\overline{\overline{ERR}}(\underline{x}(k)) - \overline{\overline{ERR}}(\underline{x}(k)+\underline{h}(k)) \ge \rho_1(\hat{ERR}(\underline{x}(k)) - \hat{ERR}(\underline{x}(k)+\underline{h}(k)) \quad \rho_1 \le 1 \tag{14}$$

If not the linear approximation is insufficient, the value of $\lambda(k+1)$ will be decreased:

$$\lambda_{k+1} = \rho_2 \lambda_k \qquad \rho_2 \prec 1 \tag{15}$$

The iterations will be stopped if one of the following criteria is reached:

a) The maximum of the function of error is lower than a certain value.

b) The maximum of $\left\|\underline{h}\right\|$ becomes very weak compared to the $\left\|\underline{x}\right\|$.

An 8-element with half wavelength element spacing is used at ISM band.

A number of examples (Table I and II) will be shown to illustrate the capabilities of this method.

The first example (Example #1) concerns the phase-only synthesis for steering lobe with one interfering in a privileged angular zone using a general synthesis method. The second example (Example #2) concerns the phase-only synthesis for multiples steering lobes in desired directions.

So, we present various cases of syntheses of linear antenna array at desired pattern to illustrate the various possibilities offered by the optimization method in order to prove the effectiveness and the flexibility of the this numerical tool.

The synthesized patterns are as follows:

- Steering lobe with one interfering in a privileged angular zone (direction of interference).
- Two steering lobes in two desired directions are shown in Figs 6, 7 and 8.

Synthesized weightings are deferred in Tables 1 and 2.

Table 1
Excitations For Different Steering Lobes And Interfering Nulling

Example #1	SYNTHESIZED VOLTAGES (Phase (Deg)), EXAMPLE #1		
	-50°(steering) and – 10°(interfering)	-40°(steering) and 50°(interfering)	-10°(steering) and 30° (interfering)
Element #	Phase (Deg) Fig.4	Phase (Deg) Fig.5	Phase (Deg) Fig.6
1	225	335	60
2	35	60	85
3	155	195	50
4	280	315	20
5	80	45	340
6	205	165	310
7	325	300	275
8	135	25	300

Table 2
Excitations For Different Multiple Steering Lobes

Example #2	SYNTHESIZED VOLTAGES (Phase (Deg)) , EXAMPLE #2		
	-20 and 40°(steering)	-60° and 50°(steering)	-30° and 30° (steering)
Element #	Phase (Deg) Fig.7	Phase (Deg) Fig.8	Phase (Deg) Fig.9
1	95	155	5
2	245	340	185
3	225	170	180
4	15	355	360
5	345	5	360
6	135	190	180
7	115	20	175
8	265	205	355

Figs 2, 3, 4 and 5 show the examples of some beamforming scenarios with interfering null steering stages to reject the in-beam interferers within the mainlobe when there exist interferers [5].

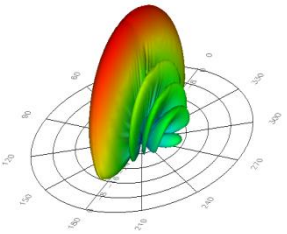

Figure 2. Steering lobe (@ 0°)

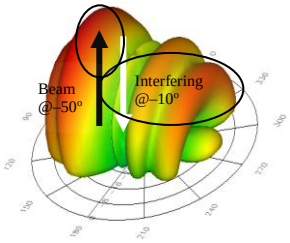

Figure 3. Steering lobe (@-50°) and interference nulling (@-10°)

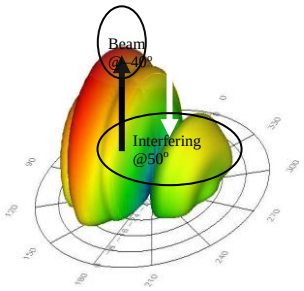

Figure 4. Steering lobe (@-40°) and interference nulling (@50°)

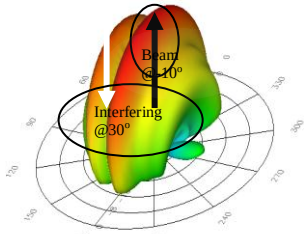

Figure 5. Steering lobe (@-10°) and interference nulling (@30°)

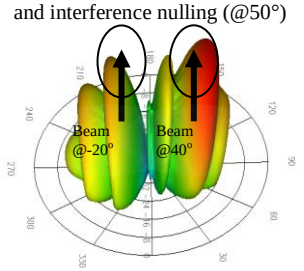

Figure 6. Two steering lobes at (@-20°)and(@40°)

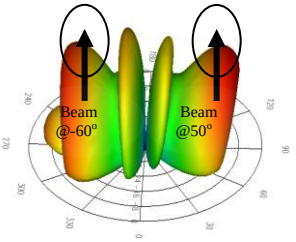

Figure 7. Two steering lobes at (@-60°)and(@50°)

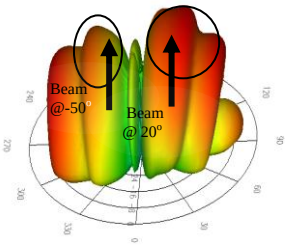

Figure 8. Two steering lobes at (@-50°)and(@20°)

3. Multilayer Networks And Back-Propagation Algorithm

Much early research in networks was abandoned because of the severe limitations of single layer linear networks. Multilayer networks were not "discovered" until much later but even then there were no good training algorithms [10]. It was not until the 80 that back-propagation became widely known.

3.1. Method of Training: Backpropagation

Define a cost function (e.g. mean square error)

$$E = \frac{1}{2L}\sum_{k=1}^{L}\left[t^{(k)} - \varphi^{(k)}\right]^2 \qquad (16)$$

Where $\varphi^{(k)}$ is the network output, $t^{(k)}$ is the desired output, the activation φ at the output layer is given by

$$\varphi = f(Wz) = f_2\left(Wf_1(wx)\right) \qquad (17)$$

and where

z is the activation at the hidden nodes.

f_2 is the activation function at the output nodes.

f_1 is the activation function at the hidden nodes.

3.2. Implementing Backpropagation

Create variables for:

- The weights W and w,
- The *net* input to each hidden and output node, net_i
- The activation of each hidden and output node, $\varphi_i = f(net_i)$
- The "error" at each node *i*.

For each input pattern *k*:

Step 1: Foward Propagation

Compute net_i and φ_i for each hidden node, *i=1,..., h*:

$$net_i = \sum_{r=1}^{n} w_{ri}x_r \text{ and } z_i = f_i(net_i) \qquad (18)$$

Where $x_1, x_2,..., x_n$ are the input signals; $w_{r1}, w_{r2}, ..., w_{rn}$ are the synaptic weights converging to neuron *i*; net_i is the cumulative effect of all the neurons connected to neuron *i*.

Compute net_j and φ_j for each output node, *j=1,..., m:*

$$net_j = \sum_{i=1}^{h} w_{ij}z_i \text{ and } \varphi_j = f_2(net_j) \qquad (19)$$

Step 2: Backward Propagation

Calculate the error terms (δ_{1j} and δ_{2j})of the nodes in the output and hidden layers, starting from the output layer and continuing with the hidden layers, moving backwards from the output layer to the input layer of the neural networks structure. The error terms are calculated according to eq.20 and eq.21.

Compute for each output node, *j=1,..., m:*

$$\delta_{2j} = (\varphi_{dj} - \varphi_j)f_2'(net_j) \qquad (20)$$

Compute for each hidden node, *i=1,..., h:*

$$\delta_{1j} = f_1'(net_i)\sum_{i=1}^{m} w_{ij}\delta_{2j} \qquad (21)$$

Where $f_1'(net_i)$ and $f_2'(net_j)$ present the derivative of the activation function.

Step 3: Accumulate gradients over the input patterns (batch)

$$\frac{\partial E}{\partial w_{ij}} = \frac{\partial E}{\partial w_{ij}} + \delta_{2j}z_i$$
$$\frac{\partial E}{\partial w_{ri}} = \frac{\partial E}{\partial w_{ri}} + \delta_{1i}x_r \qquad (22)$$

Step 4: After doing *steps 1 to 3* for all patterns, we can now update the weights:

$$w_{ij}(k+1) = w_{ij}(k) - \frac{\mu}{L}\frac{\partial E}{\partial w_{ij}}$$
$$w_{ri}(k+1) = w_{ri}(k) - \frac{\mu}{L}\frac{\partial E}{\partial w_{ri}} \qquad (23)$$

Where $\frac{\mu}{L}$ is a constant of proportionality called the learning rate.

3.3. Neural architecture

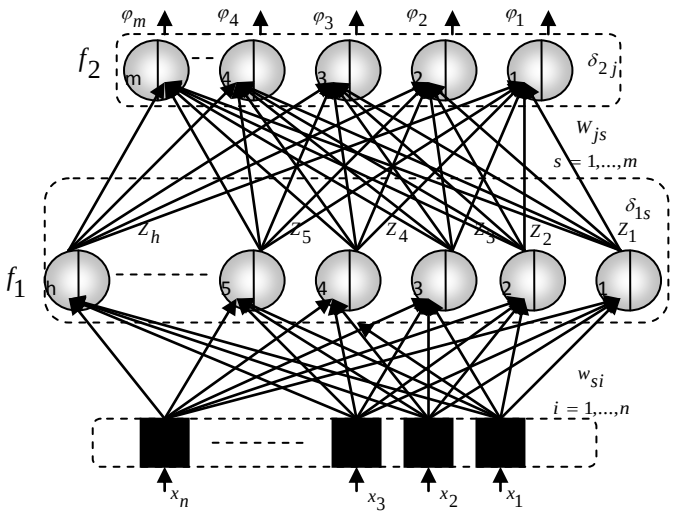

Figure 9. The neural beamformer architecture

As it was shown theoretically that a multi-layer neural network with only one hidden layer is able to identify a nonlinear function arbitrarily complexes and its derivative, our network thus contains only one hidden layer. The choice of the number of hidden neurons is strongly related to the nature of non linearity to model. In our case (Table IV), 60 hidden neurons allowed a good convergence of the algorithm and a good precision of the formed neuronal model of two entries and eight exits. The neuron used in this network is the continuous nonlinear neuron whose function of activation is a tan sigmoid function).

The architecture of a three-layer neural network, shown in Fig 9, consists of an input layer, a hidden layer and an output layer of summation nodes. The input nodes receive the pre-processed antenna data and broadcast the input vectors to each hidden layer node [10]-[11].

To investigate the ideas presented in the previous section, the first step is dividing the space in 17 sectors; repeat every 10 degrees in the interval from -85 degrees to +85 degrees inclusive. More accurate space division sectors can be reached by increasing the number of element arrays. The input vector to the entry of neural network $x = \left[x_1, x_2, ..., x_{17}\right]^T$ is in the form of a 17 bit binary code (one bit for each sector); all of the bits were set to interfering except one (+1) or two (+1 and -1). A bin input of (+1) indicates a source exactly on (main lobe) in the sector, the bin location of (0) represents no source in the sector and the bin location of (-1) indicates a null interfering in the sector. This step has the advantage to decrease considerably the number of unknown variables. Convergence may then be achieved more rapidly.

The proposed scheme (Fig.10) has been tested with excellent results, as it is shown in the following examples (examples # 1&2). An 8 element antenna array with centers separated is now used for synthesis purposes considering voltages with constant amplitude and variable phase [11].

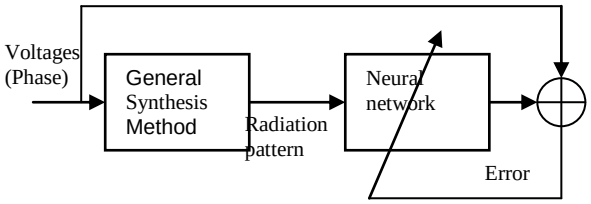

Figure 10. Neural network training procedure.

Table 3 Activation Function

Parameters	Symbol	Function
the activation function at the hidden nodes	f_1	*Sigmoid tan*
the activation function at the output nodes	f_2	*Sigmoid tan*

Table 4 Typical Values of Parameters Use In Back-Propagation Algorithm

Parameters	Symbol	value
Neuron in the input layer	n	17
Neuron in the output layer	m	8
Neuron in the hidden layer	h	60
coefficient of training	η	0.02

4. The Novel Design Of Phased Antenna Array

In this section, a description of the system model used in the simulation and the analytical study is presented. The model includes neural model, digital beamforming, phased shifter, antenna array.

4.1. Neural model

After having developed the model of controlled phase shifter (PS), one proceeds in what follows has the implementation of the phases synthesized by our neuronal model.

There is several technique of implementation which one can gather according to two large families: analogical and numerical implementation. The analogical implementation offers the advantage of a minimal surface of silicon compared to the numerical implementation. The latter has the advantage of a high degree of accuracy of calculation; we are interested in what concerns us with the numerical implementation of the phases synthesized by our neuronal model.

In work concerning the development of the numerical implementation of the model at base of Artificial Neural Networks ANNs was proposed in the form of a program structured out of assembler carried out by a microcontroller, each neuron is presented by under program or calculation is made neuron by neuron and layer by layer by a sequential process [12]-[15]. The disadvantage of this method lies in the computing time which is very significant In our case we propose a parallelization of the process by a circuit FPGA, in this case, the phases synthesized by the neuronal model in the various cases (a lobe, a lobe and interfering and two lobes) are stored in storage blocks what offers a weak computing time compared to the implementation on microcontroller or on FPGA.

So the implementation of the neural network was simulated in material form in a circuit FPGA by the means of Very High Speed Integrated Circuit Hardware Description

Language VHDL. For the implementation and the establishment of the networks of neurons of the control circuit of phase-converters we considered the solution of the parallelization of storage blocks in three cases (only one lobe, a lobe and interfering (zero) and two lobes). The Fig. 11 illustrates the diagram of the control circuit implement on FPGA.

One will treat in this paragraph the implementation on silicon of a control circuit after having fixed the network architecture of neurons to be implemented and makes the choice of the various bits of coding of the data as well as the synaptic weights and the function of activation. General architecture material proposed and the various choices of the blocks and operators implemented are defined in what follows. Finally the stage of synthesis on circuit FPGA will be started.

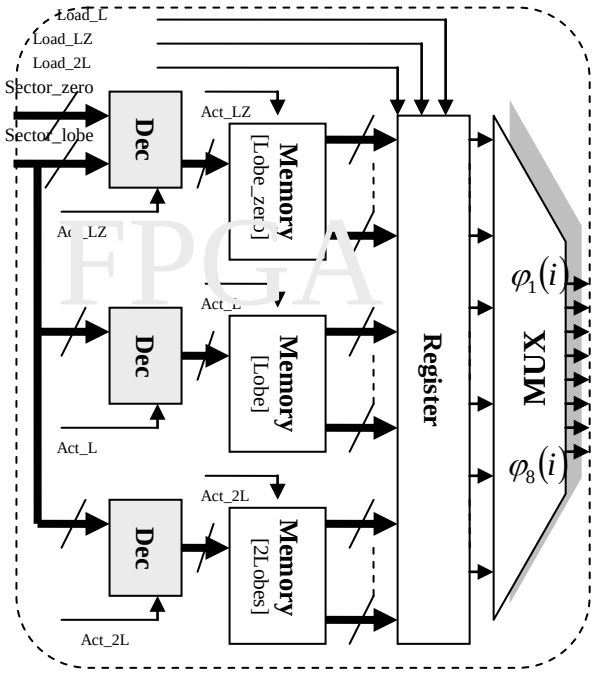

Figure 11. Neural model

The architecture of the complete neural model is shown in Fig.11 . The same is implemented using Xilinx XC3S500-4fg320 Chip. The results obtained for a 17 input neuron and 8 output neurons are shown in Table V. The architecture used 38 blocks input-output on a total of 232 (16%), it occupied 2620 SLICES on a total of 4656 (i.e. 56%) of the circuit. The response time of this structure is of 153.44ns and the work frequency of this architecture is 4 MHz.

Table 5 Resource And Timing Of Neural Model

XC3S500-4fg320	
Nb of Slices	2620 / 4656 → 56%
Nb of Bascules D	373 / 9312 → 4%
Nb of IOBs	38 / 232 → 16%
Nb of LUTs	4681/9312 → 25%
Nb of GCLKs	1/ 24 → 4%

The neural network NN based on back-propagation algorithm is implemented in FPGA. The Neural Network with 8-bit precision has been implemented using Xilinx 8.1i, simulated with ModelSim SE 6.0, and downloaded and tested in the IC 'XC3S500-4fg320'.

The neural beamformer architecture consists of antenna measurement input pre-processing, an artificial neural network, and output post-processing. This briefly summarizes the purpose and interaction of these functional elements.

Network pre-processing exploits antenna expertise to simplify and enhance neural network inputs. It removes redundant or irrelevant information, eliminates artificial discontinuities in the input function space, and reduces problem inputs to a small set of relevant information. Although neural networks can learn to ignore irrelevant inputs, and discontinuities can be trained "across", if their locations are known and boundary points are available, these techniques usually create larger (and slower) networks than ones which utilize intelligent pre-processing.

In the problem of synthesis, the amplitude of the received signal is not a strong indicator of the Direction-Of-Arrival DOA. The absolute phase of the received signal at each element also contains nonessential information. There is, however, a strong relationship element phases and Direction-Of-Arrival DOA.

We pre-process the measured phases at each element to determine the phase differences between consecutive array elements. However, these phase differences contain artificial discontinuities caused by phase transitions (or branch cuts) in received phased difference measurements from -85 degrees to +85 degrees. Discontinuities make it difficult for the network to learn the mapping from a small discrete set of training point, especially since the branch cuts are quasi-random (dependent on arbitrary receiver phase references). To eliminate the branch cuts, we use the sine and cosine of the phase differences as final processed inputs.

4.2. Antenna array

The proposed scheme has been tested with good results. An 8 element collinear half-wavelength (band 2 to 2.7 GHz) quasi-yagi array with centers separated is now used for synthesis purposes considering voltages with variable phase. The geometry of the quasi-yagi array and its feeding system with all the geometrical parameters is shown in Fig.13. The final dimensions of the circuit are:

$W_1 = W_3 = W_4 = W_5 = W_{Dir} = 3.16$ mm;
$W_6 = S = 1.58$ mm;
$W_{Dip} = 4$ mm;
$S_{Ref} = 25$ mm; $S_{Dri} = S_{Dir} = 19$ mm;
$L_{Dri} = 54$ mm; $L_{Dir} = 24$ mm ; $L_{Ref} = 65$ mm.

These dimensions have been obtained after optimisation of the total circuit. As the microstrip to coplanar stripline transition exhibits good characteristics, only the antenna geometry and the coplanar stripline dimensions have been adjusted manually. The following sub-sections reports the characteristics of the optimum antenna in terms of input impedance response and radiation characteristics [14].
The optimized antenna was simulated on an infinite substrate with the Advanced Design system 2002.

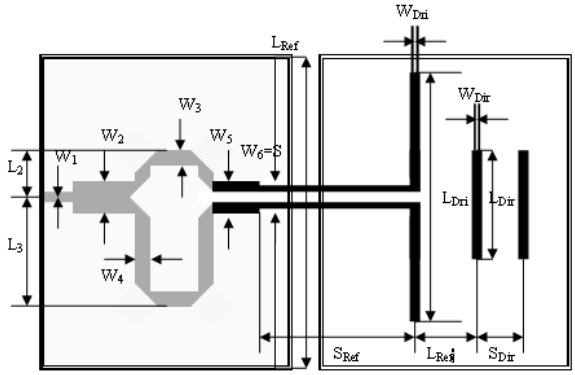

Figure 12.Geometry of the quasi-yagi antenna

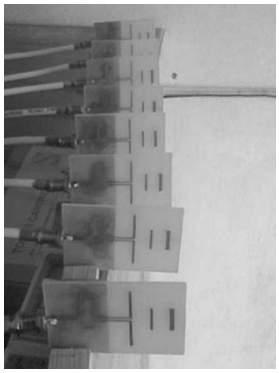

Figure 13. 8-Element prototype

In the experiment, however, pattern measurements were carried out in a fixed azimuth plane, i.e., the linear antenna array was used having a linear array of eight quasi-yagi antenna elements has been realized and tested for 3 cases of steered beams with null control, and 3 cases of multibeams. We used variable phase-shifters to control the various values of phases. The radio frequency was in the band (2.45GHz).

4.3. C. Phased Antenna Array

We present in this section an electronic platform dedicated to the implementation of a phased antenna array. We initially raise our step of design of a chart of order containing Spartan-3E. Our approach here aims at a generic architecture, dynamically reconfigurable allowing the direct implementation of the phases synthesized on a Spartan-3E able to support all the cases of synthesis of radiation pattern (a directing lobe only, a directing lobe and interfering, two directing lobes). The Control circuit is elaborate in the form of a intellectual property coded in VHSIC Hardware Description Language VHDL and synthesizable on Field Programmable Gate Array FPGA.

In the second time, two principal aspects are developed in this section, a general presentation of the material constitution of the prototype of intelligent communication, its operation and its implementation with techniques of modulations. On the basis of this base, some concrete applications are proposed and allow a practical and progressive initiation the digital processing of antennas according to the various hierarchical levels definite (Fig.14). From the various enumerated technical solutions, we can establish synoptic Xilinx Spartan-3E where the central component is the XC3S500-4fg320 [4].

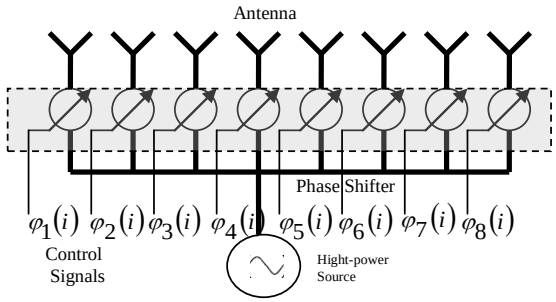

Figure 14. Conventional approach for an electronically scanned transmitter.

Fig. 15 shows a simplified phase-array transmitter that uses LO phase shifting. Phase shifting at the LO port is advantageous in that the phase-shifter loss does not directly deteriorate the transmitter sensitivity [4].

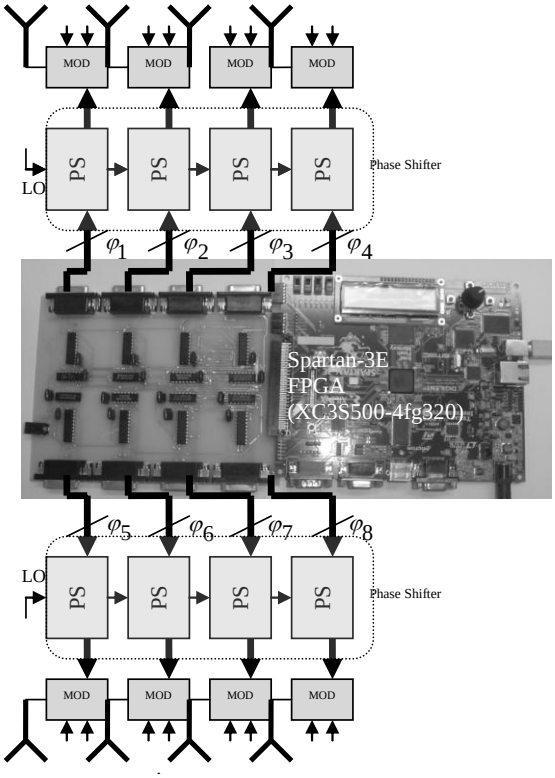

Figure 15. Block diagram of the fully integrated 2.45-GHz phased-array transmitter.

Two reasons proved the implemented of phased-array transmitter employs an LO phase-shifting architecture.

The first has been the phase shifting and signal processing was eliminated due to the larger chip area, power consumption, and and the second the high demand on the base band digital interface, particularly for the high data rates of interest.

Additionally, the Fig 15 shows the block diagram of a digital beamforming comprised of a 2.45 GHz integrated antenna array, phase shifter, modulator.

A eight-bit phase shifter gives eight possible phase states, starting at 0 degree with a 2.83 degree step.

Experiments were conducted in a radio anechoic chamber to test the basic performance of the proposed approach. An antenna system developed for application to communications was used in the experiment. The basic capabilities of beam steering and tracking were tested assuming static or mobile

conditions.

To demonstrate the performance of the method described in the previous section for steering beam and multiple beams in desired direction, and imposed null in the direction of interfering signal by controlling the phase excitation of each array element, several examples of uniform excited linear array with half wavelength spaced isotropic elements were performed.

Allowing amplitude and phase variations of the synthesized voltage values usually implies different attenuation and phase values feeding the radiating elements as, for example, the use of variable attenuators and phase shifters in the feeding network of the array antenna [16]-[17]. In practice many array problems cannot consider the use of variable attenuators, mainly because of losses, space availability, and cost as well as other design constrains, so the excitations applied to the radiating elements are required to have constant amplitude, being the phase the only variable parameter.

In this technique, the adaptive array can track the signals, and allocate beams in the direction of the of use signal while simultaneously nulling unwanted sources of interference [5].

The results presented in Fig.16 and Fig.17 show measured and simulation radiation patterns with interference nulling (at 30o and -50o respectively), while maintaining main lobes in the direction of useful signal (at 0o) for the reference antenna (8 elements antennas array) [5].

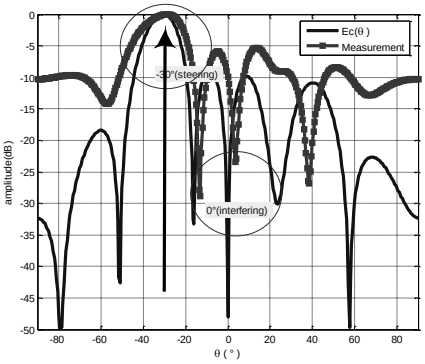

Figure 16. Steering lobe (-30°) and interference nulling (0°)

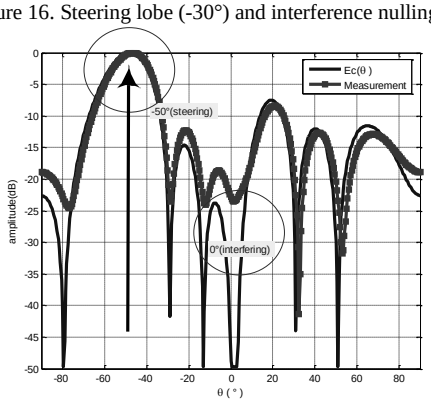

Figure 17. Steering lobe (-50°) and interference nulling (0°)

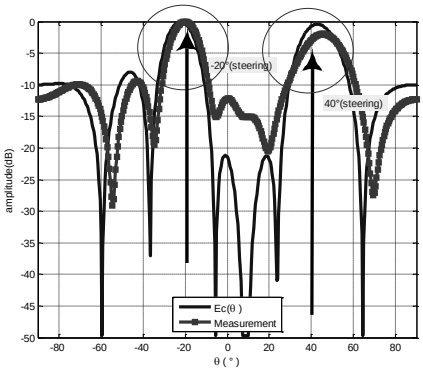

Figure 18. Two Steering lobes (-20°) and (40°)

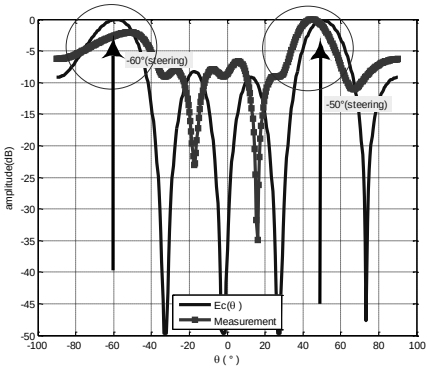

Figure 19. Two Steering lobes (-60°) and (40°)

The results of measurement of the radiation pattern in Figs. 16, 17, 18 and 19) show a very good agreement with theoretical simulation. Positions of the pointed lobe and the interfering correspond perfectly well to those envisaged by the synthesis. One gone up of the sidelobe level and of the values of the interfering could be justified by the inaccuracy in the realization of various values of the phases. The difference between the theoretical and practical values of the profit is due to the loss of insertion of feeding circuit.

So, this figures show good agreement between the simulation and the measurement results in terms of accuracy, efficiency and reliability of the model. We can see that a broad null is easily available. It is interesting to note that the method allows the control of nulling level to the detriment of the adjacent side lobes energy, which is pushed up. Also, solutions with 2 lobes are shown Figs. 18 and 19 can be reached with acceptable solutions. This algorithm does not only hold the examples presented above, but also appears to be general for all cases of synthesized desired characteristics of steered beams.

5. Conclusion

A synthesis method for the digital beamforming using the phase only control with neural network has been presented.

In this paper, we explore prototyping options and implementation of a novel design of phased antenna array using neural network with Field Programmable Gate Array. The implementation is based on a multilayer perceptron with a hardware back-propagation algorithm. It is shown that even with relatively modest FPGA devices; the architecture attains the speeds necessary for real-time training in beamforming applications.

The dynamically phased arrays make use of the Direction-Of-Arrival DOA information from the desired user

to steer the main beam towards the desired user. The signals received by each antenna element are weighted and combined to create a beam in the direction of the mobile. Only the phases of the weights are varied and the amplitudes are held constant. We have described an iterative technique, which is able to compute the desired pattern for antenna arrays by modifying only the phase excitations. The proposed approach can be easily implemented without complicated mathematical programming methods. Therefore, the usage of back-propagation algorithm to reduce errors shows very interesting results, even though if, considering the approximations for bias and noise, they would have to be verified according to the application environment.

Acknowledgment

The authors wish to acknowledge the constructive comments and suggestion provided by the reviewers. Their kind effort certainly contributed to the quality of this publication. This work was supported by the Lebanese University research project.

References

[1] J.Costantine, K.Y. Kabalan, A.EI-Hajj, and M.Rammal, "New Multi-Band Microstrip Antenna Design for Wireless Communications," IEEE Antennas and Propagation Magazine, Vol. 49, No. 6, pp.181-186, 2007.

[2] T.B. Vu, "Simultaneous Nulling in Sum and Difference Patterns by Amplitude Control," IEEE Trans. Antennas and Propagation, Vol. AP-34, pp. 214-218, 1986.

[3] T.William, Z.Salcic, S.K.Nguang, "Prototyping Neuroadaptive Smart Antenna for 3GWireless Communications," EURASIP Journal on Applied Signal Processing, pp.1093–1109, 2005.

[4] R. L. Haupt, "Phase-only adaptive nulling with a genetic algorithm", IEEE Trans. Antennas Propagat, Vol. 45, pp. 1009-1015, 1997.

[5] N. Fadlallah, M. Rammal, H. Rammal, P. Vaudon, R. Ghayoula, A. Gharsallah, "General synthesis method for linear phased antenna array", IET Microw. Antennas Propag., Vol. 2, No. 4, pp. 338–342, 2008.

[6] Varlamos, P. K. and C. N. Capsalis, "Electronic beam steering using switched parasitic smart antenna arrays," Progress In Electromagnetics Research, PIER 36, 101–119, 2002.

[7] J. L. Cruz, B. Ortega, M. V. Andres, B. Gimeno, J. Capmany, and L. Dong, "Array Factor of a Phased Array Antenna Steered by a Chirped Fiber Grating Beamformer", IEEE Photonics Technology Letters, Vol.10,No.8, Aug 1998.

[8] M.Rammal, D.Eclercy, A.Reineix, B. Jecko, "Comparaison between real and power optimisation methods for arrays synthesis of antennas", Electronics Letters, Vol. 32, No 2, 3 January 1996.

[9] K. Madsen, "An Algorithm for Minmax Solution of Over Determined Systems of Nonlinear Equations", J. INS. Math. Appl.,Vol.16, pp. 321-328, 1975.

[10] R.Ghayoula, N.Fadlallah, A.Gharsallah, M.Rammal, "Neural Network Synthesis Beamforming Model for One-Dimensional Antenna Arrays", The Mediterranean Journal of Electronics and Communications, ISSN: 1744-2400, Vol. 4, No. 1, pp.126-131, 2008.

[11] G. A. Rafael, L. H. Fernando, L. F. Herrán, "Neural Modeling of Mutual Coupling for Antenna Array Synthesis", IEEE Trans. Antennas Propagat., Vol. 55, pp. 832-840, 2007.

[12] Robert R. Romanofsky, Jennifer T. Bernhard, Frederick W. Van Keuls, Félix A. Miranda, Gregory Washington, and Chadwick Canedy "K-Band Phased Array Antennas Based on $Ba_{0.60}Sr_{0.40}TiO_3$ Thin-Film Phase Shifters", IEEE Tran. On Micowave Theory and Techniques, Vol. 48, No. 12, pp. 2504- 2510, 2000.

[13] S. A. Zekavat and C. R. Nassar, "Smart antenna arrays with oscillating beam patterns: characterization of transmit diversity using semi-elliptic coverage geometric-based stochastic channel modeling," IEEE Trans. Commun., Vol. 50, pp. 1544–1556, Oct. 2002.

[14] V.Van Yem, "Conception et réalisation d'un sondeur de canal multi-capteur utilisant les corrélateurs cinq-ports pour la mesure de propagation à l'intérieur des bâtiments", École Doctorale d'Informatique, Télécommunications et Électronique de Paris, Thèse de Doctorat, Dec.2005.

[15] J.Ramesh, P.T.Vanathi, and K.Gunavathi, "Fault Classification in Phase-Locked Loops Using Back Propagation Neural Networks", ETRI Journal, Vol.30, Nb 4, pp.546-554, 2008.

[16] F. Glover, "Tabu Search-part I," ORSA Journal on Computing, Vol. 1, pp. 190-206, 1989.

[17] F. Glover, "Tabu Search-part II," ORSA Journal on Computing, Vol. 2, pp. 4-32, 1990.